



저작자표시-비영리-변경금지 2.0 대한민국

이용자는 아래의 조건을 따르는 경우에 한하여 자유롭게

- 이 저작물을 복제, 배포, 전송, 전시, 공연 및 방송할 수 있습니다.

다음과 같은 조건을 따라야 합니다:



저작자표시. 귀하는 원저작자를 표시하여야 합니다.



비영리. 귀하는 이 저작물을 영리 목적으로 이용할 수 없습니다.



변경금지. 귀하는 이 저작물을 개작, 변형 또는 가공할 수 없습니다.

- 귀하는, 이 저작물의 재이용이나 배포의 경우, 이 저작물에 적용된 이용허락조건을 명확하게 나타내어야 합니다.
- 저작권자로부터 별도의 허가를 받으면 이러한 조건들은 적용되지 않습니다.

저작권법에 따른 이용자의 권리는 위의 내용에 의하여 영향을 받지 않습니다.

이것은 [이용허락규약\(Legal Code\)](#)을 이해하기 쉽게 요약한 것입니다.

[Disclaimer](#)

Thesis for the Degree of Master of Science

Automatic determination of seismic phase arrival times

by

Minook Kim

in Division of Earth Environmental System Science

(Major of Earth & Environmental Sciences),

The Graduate School,

Pukyong National University

August 2016

Automatic determination of seismic
phase arrival times
(지진파 위상 도착시간 자동 결정)

Advisor: Prof. Tae-Seob Kang

by
Minook Kim

A thesis submitted in partial fulfillment of the requirements
for the degree of

Master of Science

in Division of Earth Environmental System Science
(Major of Earth & Environmental Sciences),
The Graduate School,
Pukyong National University

August 2016

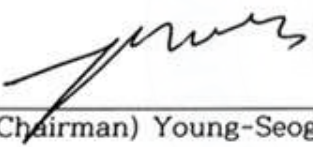
Automatic determination of seismic phase arrival times

A dissertation


by

Minook Kim

Approved by:



(Chairman) Young-Seog Kim



(Member) Junkee Rhie



(Member) Tae-Seob Kang

August 2016

CONTENTS

List of Figures	vi
List of Tables	ix
Abstract	x
I . Introduction	1
II . Theory and Method	5
1. Methods for determination of seismic phase arrival-time	5
(1) Earle and Shearer's method (ESM)	
(2) Modified Allen's method (MAM)	
(3) Modified Baer and Kradolfer's method (MBKM)	
(4) Comparison of three autopicking methods	
2. Initial event declaration	12
3. Automatic picking of P-phase arrival-time	14
4. Rotation of three-component seismograms	18
5. Automatic picking of S-phase arrival-time	22

6. Final event declaration	25
III. Data and Result	28
1. Seismic network	28
2. Data	32
3. Determination of hypocenter	35
IV. Discussion and Conclusion	43
Reference	45
국문 초록	48

List of Figures

Fig 1. Indiscernible signature of P- and S-wave arrival times due to low signal-to-noise ratio in microseismic waveforms.	4
Fig 2. Examples of automatic picking of P-wave arrival time in comparison with manual picking. Red line indicates manual, purple one Earle and Shearer (ES), green one Allen (CF), and blue one Baer and Kradolfer (BK), respectively.	11
Fig 3. Initial declaration of event. Detection threshold and criterion of the STA/LTA ratio are set to 15 and 3, respectively. The event is declared when the number of stations that the STA/LTA ratio exceeds the threshold within the association window with length of six seconds is greater than the criterion. Red line denotes the threshold level and green box shows the association window.	13
Fig 4. Four steps of an automatic P-wave arrival time picking: a) Search for the maximum BK value in the saved event waveform, b) Search for the two-thirds BK value before the maximum of it, c) Set-up of a time window with length of 50 samples before the maximum BK value, and d) Assignment of P-wave phase arrival time with the sample point that the BK function starts to increase.	17
Fig 5. Calculation of the backazimuth. a) A time window with length of	

two seconds is set up, which is from -1s to +1s with reference to the P-wave arrival time. b) Each energy of E and N component is computed. c) Since the energy is an absolute value, the angle calculated using the energy ratio between two components has both the positive and negative values. d) After E and N components are rotated by using both the negative and positive angles, respectively, the angle which has more energy in N component is selected as the backazimuth. 20

Fig 6. Calculation of the incidence angle. a) The backazimuth is determined using the energy ratio between E and N components in the time window from -1 to +1 second with reference to the P-wave arrival time. b) After E and N components are rotated into radial and tangential components to the backazimuth, the incidence angle is calculated using the energy ratio of the radial and vertical components in the same way that calculate the backazimuth. 21

Fig 7. Three steps of an automatic S-wave arrival time picking: a) Search for the maximum BK value from one seconds after the P-wave arrival time, b) Set-up of a time window with length of 50 samples before the maximum BK value, c) Assignment of S-wave phase arrival time with the sample point that the BK function starts to increase. 24

Fig 8. Use of the Wadati diagram for removal of falsely determined arrival time. a) S-P time against P-wave arrival time over all stations

is plotted. b) The stations aligned in a zone with an average slope calculated using P- and S-wave velocity in the velocity model of the study area are selected as the ones with correctly determined arrival time. 27

Fig 9. A temporary broadband seismograph network which is consisting of 20 stations distributed in Jeju Island. Yellow triangle shows the location of 15 stations used in this study and red one denotes 5 stations with no available data, respectively. 29

Fig 10. Events at a range of $33^{\circ} \sim 33.7^{\circ}$ in latitude and $126^{\circ} \sim 127.1^{\circ}$ in longitude announced by Korea Meteorological Administration. 31

Fig 11. Earthquake sequence occurred in the northern offshore Jeju island on August 15, 2014. 39

Fig 12. Comparison of the epicenters determined by KMA, KIGAM, and manual picking, respectively. The event is No. 1 at Table 7. 41

Fig 13. Comparison of the epicenters determined by KMA, KIGAM, and manual picking, respectively. The event is No. 2 at Table 7. 42

List of Tables

Table 1. Comparison of time differences between manual and each three different method in picking of P-wave arrival times for 14 traces of event that occurred in north sea of Jeju island on 15 August 2014.	10
Table 2. Station information. The stations with asterisk are not used in this study due to the recording problem.	30
Table 3. Parameters for detecting event and picking arrival time. ..	33
Table 4. The averaged slope of the Wadati diagram.	34
Table 5. The 12 initial P-wave velocity structure.	37
Table 6. Source parameters of 27 events occurred in the northern offshore Jeju island on August 15, 2014.	38
Table 7. Comparison of source parameters announced by KMA and KIGAM with those determined using manual and automatic methods introduced in this study. Distance difference is a distance between epicenters determined using the automatic method and those using other methods.	40

Automatic determination of seismic phase arrival times

by

Minook Kim

Division of Earth Environmental System Science (Major of Earth and
Environmental Sciences)

Abstract

Determination of P- and S-wave phase arrival times is significant factors in microseismic detection and thus hypocenter source inversion. If analysts try to pick P- and S-wave phase arrival times of microseismic events manually, they are at risk for inconsistency in picking due to subjective determination of P- and S-wave phase arrival times among them and get to spend too much time in doing the job. This study presents a method for the automatic determination of arrival times of seismic phases. An implementation of the method is consisting of five steps. The first is the initial declaration of an event in continuous seismic data using a characteristic function which is also designed specifically in this study. The second is the automatic determination of P-wave phase arrival time using the normalized squared-envelope function. The third is the application of three-axis rotation using an energy ratio among three-component seismograms of the event. The fourth is the automatic determination of S-wave phase arrival time. The final step is the removal of falsely determined time in some records using the Wadati diagram which plots S-P times against P-wave phase arrival times over stations used in the picking stage. Application of the method to the continuous waveform data from a temporary broadband seismograph network consisting of 20 stations

distributed in Jeju Island shows that the automatic event detection and determination of phase arrival times are carried out with accuracy.



I Introduction

Determination of P- and S-wave arrival times is significant factors in microseismic detection and thus hypocenter source inversion. Microseismic is an important research method not only of oil reservoir detection (Kendall et al., 2011) and the injection process about development of the reservoir (Maxwell, 2011), but also of local seismicity due to linearity relationship between earthquake magnitude and occurrence number in accordance with Gutenberg and Richter's empirical law (Gutenberg and Richter, 1956). In case of weak signal from an event with low magnitude such as tectonic microearthquake as well as fracking-induced microseismic, an accurate determination of P- and S-wave arrival times is very difficult task because of indistinguishable event signals from background noise due to typically low signal-to-noise ratio (SNR). Also, if analysts try to pick P- and S-wave arrival times of microseismic events manually, they are at risk for inconsistency in picking due to subjective determination of P- and S-wave arrival times among them and come to consume time enormously.

Various methods of automatic event detection and seismic phase pickers has been developed up to the present. Allen (1978) developed the *STA/LTA* ratio method by using a characteristic function (CF). Munro (2004) calculated the *STA/LTA* ratio by using the energy of amplitude. Sabbione and Velis (2010) used the modified Coppers'

method. Molyneux and Schmitt (1999) used cross-correlation of amplitude. Yung and Ikelle (1997) used higher order statistics like skewness and kurtosis. Saari (1991) and Oye and Roth (2003) calculated the STA/LTA ratio of absolute value in three components. Chen and Stewart (2006) used the averaged absolute amplitude of traces in several time windows before and after each time point (sample) as the characteristic functions. Wong et al. (2009) developed a time-picking scheme for individual traces based on a modified energy ratio (MER) attribute. Earle and Shearer (1994) developed an algorithm based on the *STA/LTA* ratio taken along an envelope function. Leonard and Kennett (1999) used an auto-regressive (AR) technique. Vera-rodriguez et al. (2011) presented a method of pickers by using the blocky *STA/LTA* ratio.

Because, in general, P-wave amplitude is relatively smaller than S-wave amplitude, S-wave phase could be mistaken by P-wave phase in case of microseismic detection and determination of phase arrival time. Fig 1 shows that S-wave phase arrival is well recorded while P-wave phase arrival is indistinguishable from the background noise level. In such cases, S-wave phase arrival could be misidentified as the first arrival from an event, and then it could be a major cause of error in source inversion. Thus, accurate determination of S-wave phase arrival time is of great importance in microseismic analysis.

It is a typical observation from seismograms that P-wave recorded at a station from an earthquake is mixed by the preceding P waves and background noise, whereas S-wave is mixed by the preceding S waves, background noise, P coda waves, P_n waves, P_MP waves and so on (Lois et al., 2013). Because S waves are a mixture of many waves

more than P waves, determination of S-wave arrival time is expected to be relatively less accurate than that of P-wave arrival time in automatic seismic phase picking. In order to determine the accurate S-wave arrival time, the backazimuth to the event and the incidence angle of the wave can be calculated from the wave propagation path, and then, using those information, the three-component waveforms can be rotated in three dimension with reference to the event. However, it is difficult to calculate the backazimuth and the incidence angle before determining epicenter.

This study aims to develop an algorithm that determines the seismic phase arrival times and thus the exact hypocenter automatically. At first, the existing methods used for the automatic determination of seismic phases are reviewed, and the performance is compared among the methods with the selected waveforms from an event occurred in the northern offshore Jeju Island. Then, a new algorithm is introduced in detail. The performance test is carried out including the comparison of the detection results with those by the existing methods. Finally, the characteristics of the newly developed algorithm are discussed.

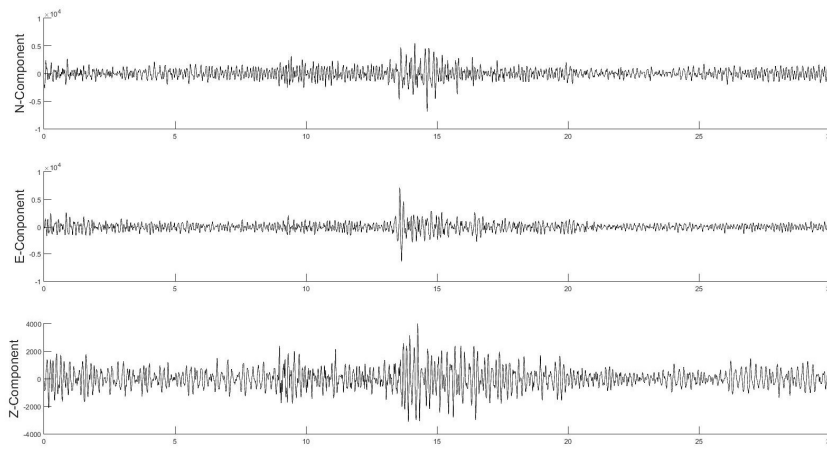


Fig 1. Indiscernible signature of P- and S-wave arrival times due to low signal-to-noise ratio in microseismic waveforms.

II Theory and Method

1. Methods for determination of phase arrival-time

In order to determine automatic arrival time of seismic phases, we compare to 3 method proposed by Earle and Shearer (1994), Allen (1978), and Baer and Kradolfer (1987). Earle and Shearer (1994) and Allen (1978) use the *STA/LTA* ratio method and Baer and Kradolfer (1987) uses the normalized squared envelope function. Comparison between 3 other methods has done in order to compare the accuracy of determination of phase arrival time from this method. This method is explained below. Table 1 represents P-wave arrival residual time of between manual picking and 3 methods picking for 14 traces of event that occurred in north sea of Jeju island on 15 August 2014. Fig 2 shows example of P-wave arrival time picking of manual and 3 methods.

(1) Earle and Shearer's method (ESM)

Phase arrival time is determined by using the STA/LTA ratio method based on envelope function (ES) proposed by Earle and Shearer (1994):

$$ES_i = \sqrt{s_i^2 + \tilde{s}_i^2}, \quad (1)$$

where s_i is the i -th signal and \tilde{s}_i is a signal applied to a Hilbert transform. The average of ES_i is computed by means of T_{STA} (shot term average window length) and T_{LTA} (long term average window length), respectively. The STA/LTA ratio is given as function:

$$\frac{STA_i}{LTA_i} = \frac{\frac{1}{N_{STA}} \sum_{j=i}^{i+N_{STA}-1} ES_j}{\frac{1}{N_{LTA}} \sum_{j=i}^{i+N_{LTA}-1} ES_j}, \quad (2)$$

where N_{STA} and N_{LTA} are length of the windows size, respectively. Method of Earle and Shearer (1994) is depicted in fig 2b.

(2) Modified Allen's method (MAM)

Phase arrival time is determined by using the STA/LTA ratio method based on characteristic function (CF) proposed by Allen (1982):

$$CF_i = S_i^2 + C_i(S_i - S_{i-1})^2, \quad (3)$$

$$C_i = \frac{\sum_{j=1}^i |S_j|}{\sum_{j=1}^i |S_j - S_{i-1}|}, \quad (4)$$

where C_i is a weighted value which represent balances in CF_i . In the CF_i , the first term relate to the energy of signal and the second term relate to the frequency of one. The average of CF_i is computed by means of T_{STA} and T_{LTA} , respectively. The STA/LTA ratio is calculated from CF_i instead of ES_i into Eq. (2). Method of Allen (1982) is depicted in fig 2c.

(3) Modified Baer and Kradolfer's method (MBKM)

Phase arrival time is determined by calculating the envelope function E_i^2 given:

$$E_i^2 = S_i^2 + \frac{\sum_{j=1}^i S_j^2}{\sum_{j=1}^i (S_j - S_{j-1})^2} (S_i - S_{i-1})^2. \quad (5)$$

Instead of the STA/LTA ratio method in time windows of averaging E_i^2 , Baer and Kradolfer (1987) proposed to calculate the normalized squared envelope function (BK) for each sample i along the trace:

$$BK_i = E_i^4 - \frac{\tilde{\mu}_{E_i^4}}{\tilde{\sigma}_{E_i^4}}, \quad (6)$$

where $\tilde{\mu}_{E_i^4}$ is mean value of E_i^4 and $\tilde{\sigma}_{E_i^4}$ is estimated standard deviation of its (Sabbione and Velis, 2013). Method of Baer and Kradolfer (1987) is depicted in fig 2d.

(4) Comparison of three autopicking methods

Methods of ESM, MAM, and MBKM for automatic determination of arrival times of seismic phases are applied to event data in study area. Table 1 represents P-wave arrival residual time of between manual picking and 3 methods picking for 14 traces of a event. Fig 2 shows example of P automatic arrival time picking of manual and 3 methods. Residual times of ESM, MAM, and MBKM are 0.126s, 0.143s, and 0.034s for 14 traces, respectively. Result of MBKM shows that determination of P-wave automatic arrival time is carried out with most accurately among 3 methods. However, calculation of BK function has disadvantage that takes a long time rather than others. Since BK function takes a long computing time to detect event in continuous seismic data, it is used only to determinate phase arrival times in event data. The CF method has considerable variations when seismic phase arrives. So, the *STA/LTA* ratio method using CF is used to detect event (Fig 2c).

Station	Residual time(s)		
	ES	CF	BK
PK01	0.035	0.030	0.000
SS02	0.265	0.190	0.105
SS04	0.185	0.290	0.115
SS05	0.015	0.175	0.095
SS10	0.050	0.100	0.070
TP01	0.075	0.075	0.000
TP02	0.125	0.120	0.005
TP03	0.030	0.030	0.005
TP04	0.270	0.270	0.040
TP07	0.220	0.220	0.005
TP08	0.015	0.015	0.020
TP10	0.145	0.145	0.010
TP11	0.265	0.265	0.005
TP13	0.070	0.130	0.030
Average	0.126	0.143	0.034

Table 1. Comparison of time differences between manual and each three different method in picking of P-wave arrival times for 14 traces of event that occurred in north sea of Jeju island on 15 August 2014.

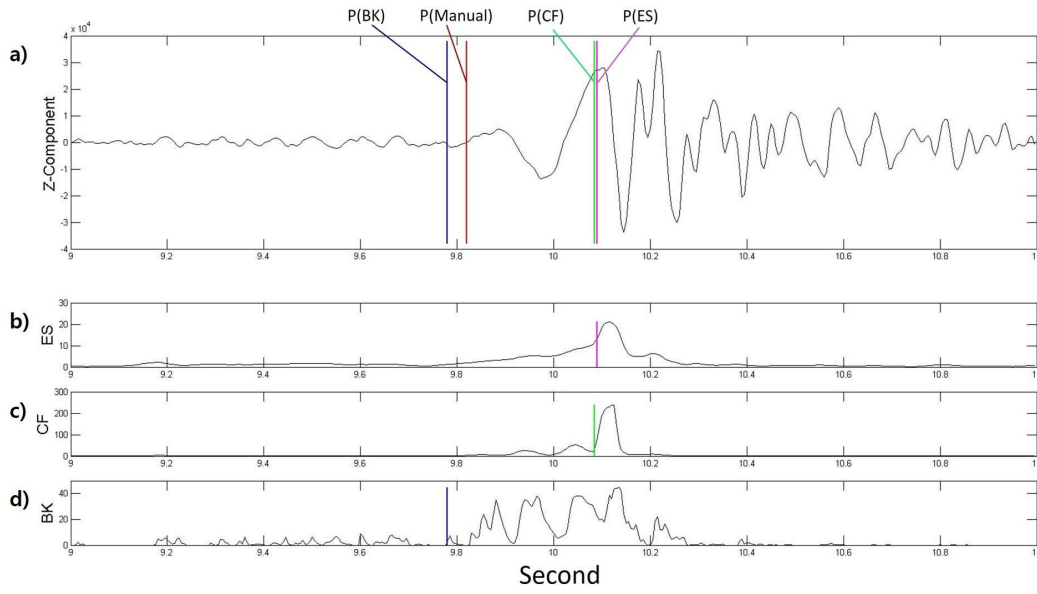


Fig 2. Examples of automatic picking of P-wave arrival time in comparison with manual picking. Red line indicates manual, purple one Earle and Shearer (ES), green one Allen (CF), and blue one Baer and Kradolfer (BK), respectively.

2. Initial event declaration

In this step, the event is detected by using the STA/LTA ratio method based on characteristic function (CF) proposed by Allen (1982). The event is declared when numbers of trace over the threshold that exceeds the STA/LTA ratio value exceed the criterion based on seismic network size within the association window. And then cut waveform is saved. The first event declaration is depicted in fig 3. The sizes of N_{STA} and N_{LTA} are depended on magnitude and frequency of event (Akram and Eaton, 2016). High the criterion and the threshold could miss the event, whereas low they could declare false event. They are based on empirical factors and depended on seismic network size.

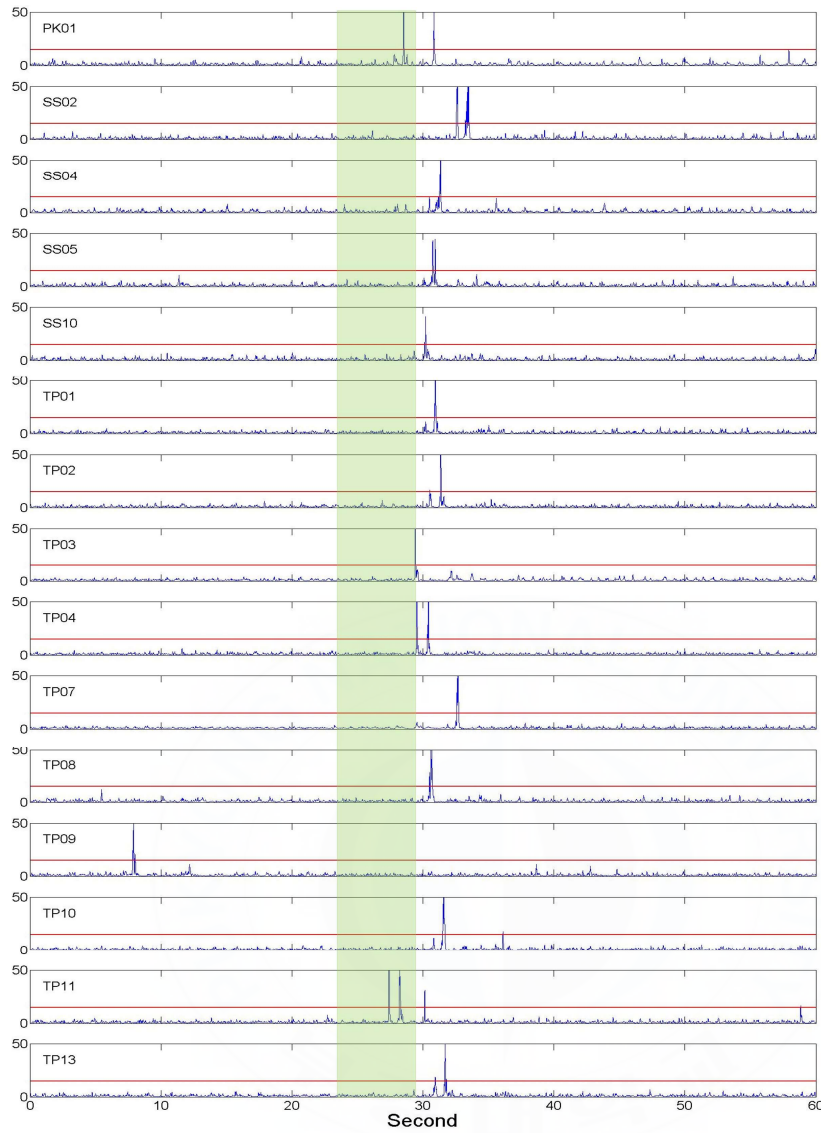


Fig 3. Initial declaration of event. Detection threshold and criterion of the STA/LTA ratio are set to 15 and 3, respectively. The event is declared when the number of stations that the STA/LTA ratio exceeds the threshold within the association window with length of six seconds is greater than the criterion. Red line denotes the threshold level and green box shows the association window.

3. Automatic Picking of P-phase arrival-time

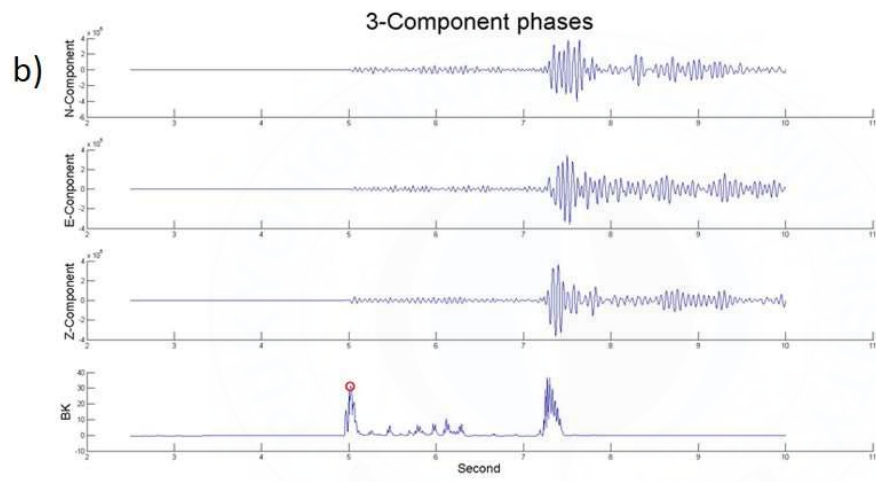
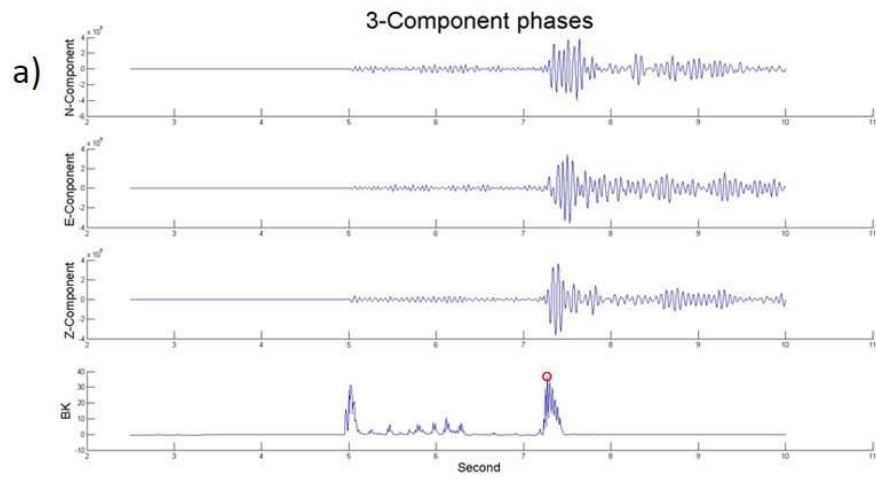
The normalized squared envelope function (BK) proposed by Baer and Kradolfer (1987) is used in order to determine automatic P-wave arrival time. The window size to the *STA/LTA* ratio method is depended on magnitude and frequency of event. The window size is significant factors in determination of automatic phase arrival time and is depended on experience of analysts. Whereas, the BK method don't need the window size contrary to the *STA/LTA* ratio method. As a result, the parameter to be consider is reduced and result of determination of automatic phase arrival time is carried out more objectively. An automatic P-wave arrival time in saved waveform is carried out over 4 steps (Fig 4) by using BK function.

1. Search for the maximum BK value. But don't know whether P-wave arrival time or S-wave arrival time (Fig 4a).
2. Search for the two-third BK value before maximum BK value. In case of absence of it, maximum BK value point is selected by P-wave arrival time (Fig 4b).
3. A 50-sampling window is set before point of maximum BK value from step 2 (Fig 4c).
4. Increasing sample point of BK function is determined by P-wave

arrival time (Fig 4d).

P-wave arrival time is determined using only Z component.





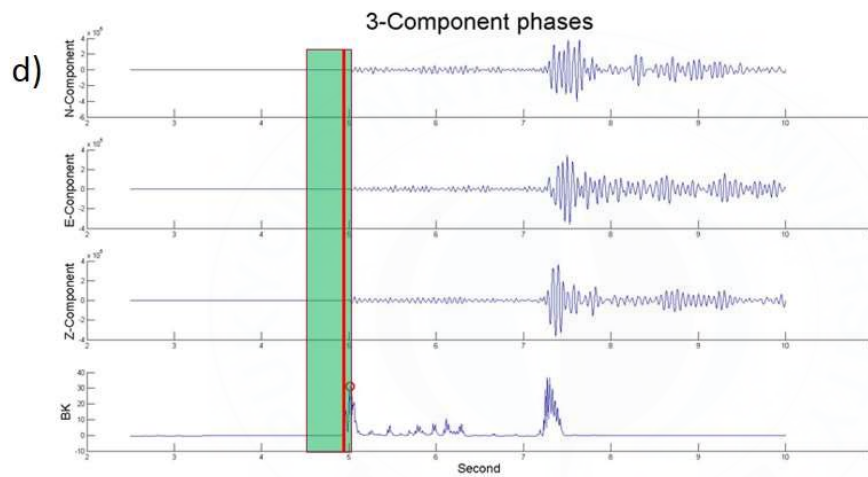
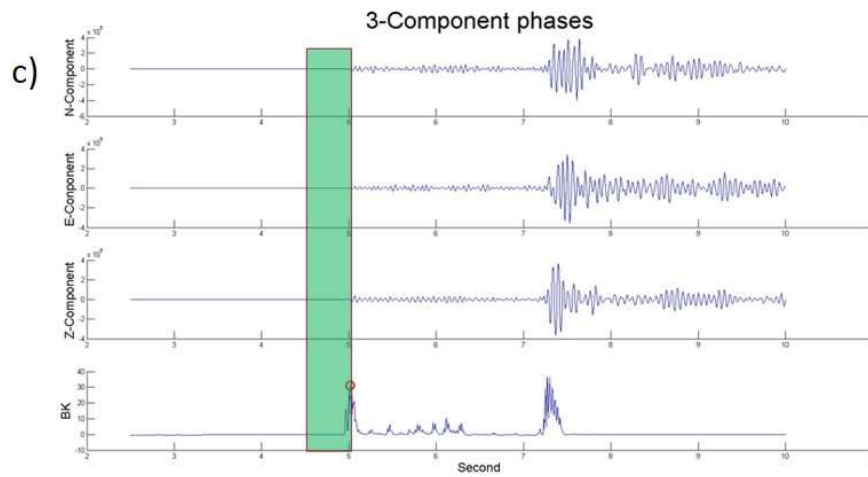


Fig 4. Four steps of an automatic P-wave arrival time picking: a) Search for the maximum BK value in the saved event waveform, b) Search for the two-thirds BK value before the maximum of it, c) Set-up of a time window with length of 50 samples before the maximum BK value, and d) Assignment of P-wave phase arrival time with the sample point that the BK function starts to increase.

4. Rotation of three-component seismograms

The motion direction of P- and S-wave phase relate to the seismic propagation path. As P-wave is compressional wave, the motion direction of P-wave match up the seismic propagation direction. Whereas, the motion direction of S-wave is perpendicular to the seismic propagation direction. More accurate S-wave phase arrival time could be determined by using the propagation characteristics of seismic phase. To do that, after computing the backazimuth and the incidence angle between station and hypocenter, rotation of three component seismograms is applied to each traces. But the backazimuth and the incidence angle could not be known before hypocenter is located. In order to determine the backazimuth and the incidence angle the new method using energy ratio of three component seismograms is developed, which is calculated by the energy of P-wave arrival time from -1s to +1s (Fig 5a, 5b).

$$E = \sum_{i=p}^{p+200} \sqrt{S_i^2 + H(S_i)^2}, \quad (6)$$

where E is energy and H is Hilbert transform. In order to calculate the backazimuth, E and N energy ratio is computed by arctangent:

$$\theta = \arctan\left(\frac{E_E}{E_N}\right). \quad (7)$$

Because the range of θ is only from 0 to 90 degree, traces of N and E component have to be rotated by positive and negative θ (Fig 5c). So, the backazimuth is determined from more energy of N component calculated by rotation of either positive or negative θ . T and R component are N and E component rotated by θ (Fig 5d).

In order to calculate the incidence angle, Z and R energy ratio is computed by arctangent:

$$\phi = \arctan\left(\frac{E_Z}{E_R}\right). \quad (8)$$

Because the range of ϕ is only from 0 to 90 degree, traces of Z and R component have to be rotated by positive and negative ϕ . So, the incidence angle is determined from more energy calculated by rotation of either positive or negative ϕ (Fig 6).

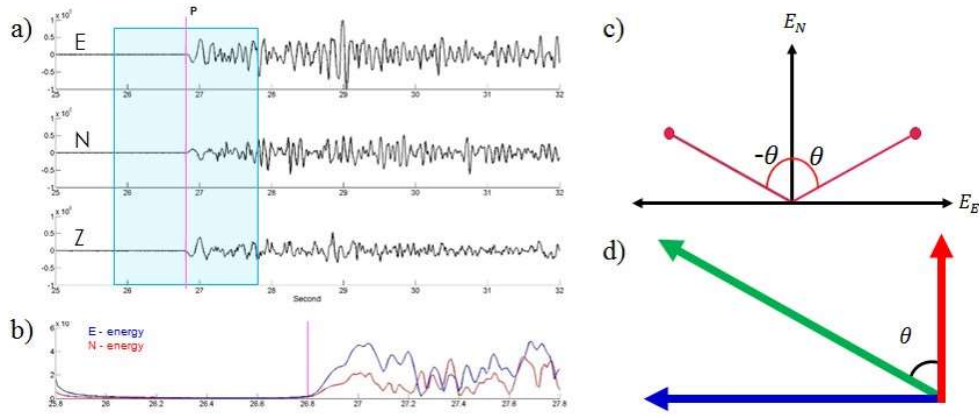


Fig 5. Calculation of the backazimuth. a) A time window with length of two seconds is set up, which is from -1s to +1s with reference to the P-wave arrival time. b) Each energy of E and N component is computed. c) Since the energy is an absolute value, the angle calculated using the energy ratio between two components has both the positive and negative values. d) After E and N components are rotated by using both the negative and positive angles, respectively, the angle which has more energy in N component is selected as the backazimuth.

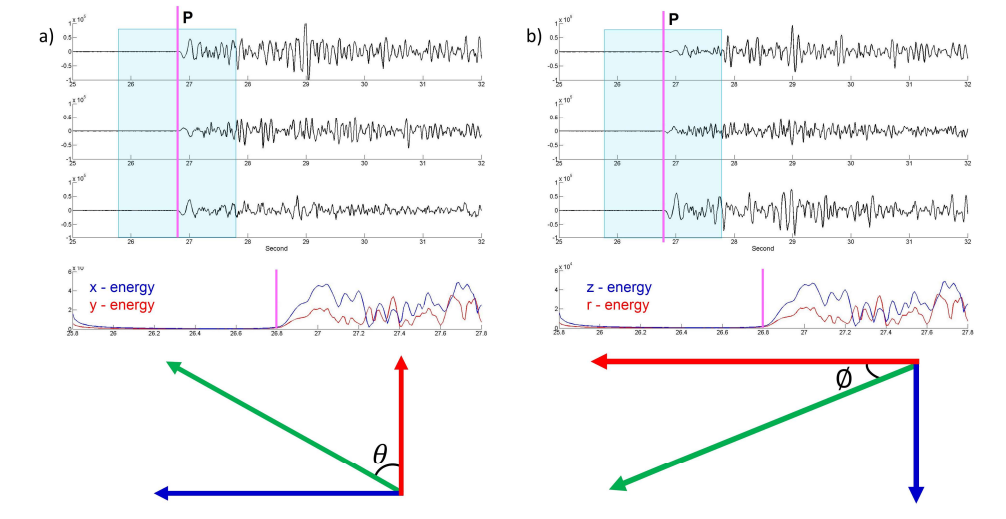


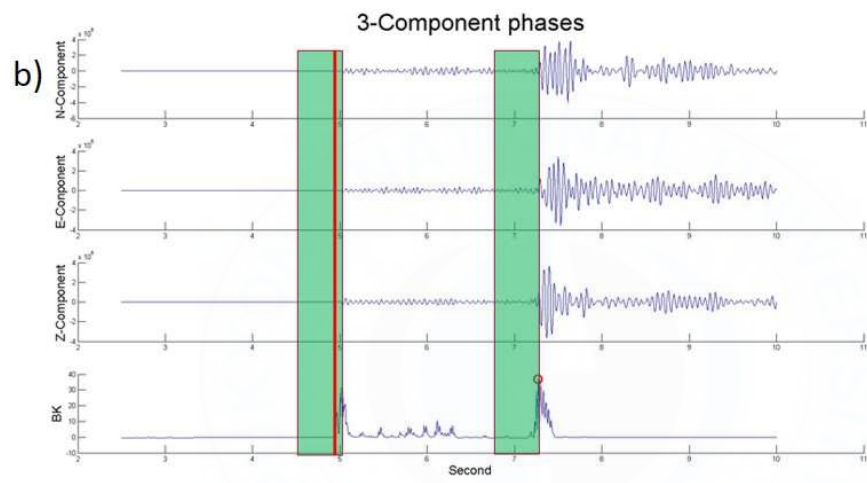
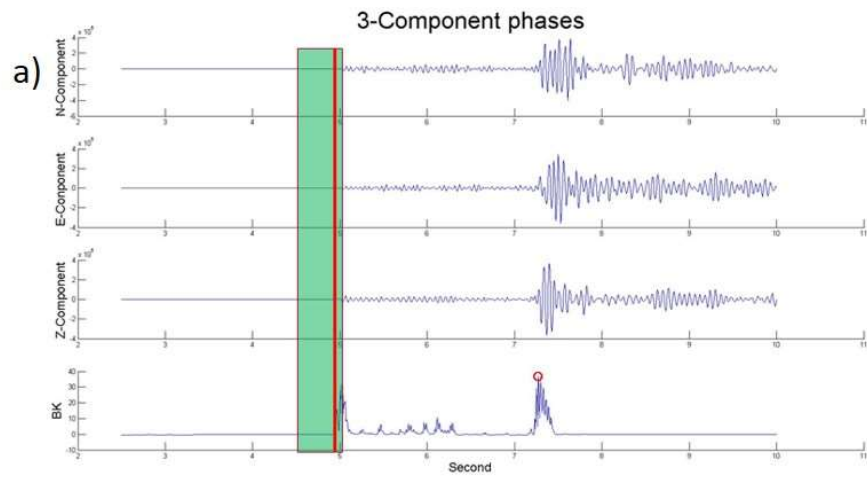
Fig 6. Calculation of the incidence angle. a) The backazimuth is determined using the energy ratio between E and N components in the time window from -1 to +1 second with reference to the P-wave arrival time. b) After E and N components are rotated into radial and tangential components to the backazimuth, the incidence angle is calculated using the energy ratio of the radial and vertical components in the same way that calculate the backazimuth.

5. Automatic Picking of S-phase arrival-time

A number of picking algorithms of phase arrival time determine P- and S-wave phase arrival time when function value exceeds a given threshold in microseismic data. However, this method have developed algorithm that determine not only P-wave but also S-wave phase arrival time automatically. Especially, if P-wave arrival phase time is only determined in microseismic analysis, S-wave phase could be mistaken by P-wave phase because P-wave amplitude is relatively smaller than S-wave amplitude. So, determination of S-wave phase arrival time is important. S-wave phase arrival time is determined by using maximum BK function since the P-wave phase arrival time. An automatic S-wave arrival time in saved waveform rotated 3-axis by using Eq. (6) is carried out over 3 steps (Fig 7) by using BK function.

1. Search for the maximum BK value after a second from P-wave arrival time (Fig 7a).
2. A 50-sampling window is set before point of maximum BK value from step 1 (Fig 7b).
3. Increasing sample point of BK function is determined by S-wave arrival time (Fig 7c).

S arrival time is determined one of faster than N or E component.



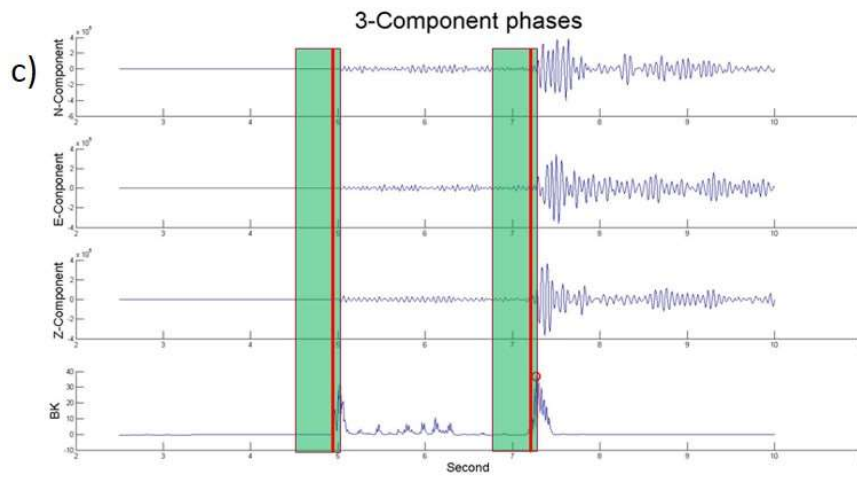


Fig 7. Three steps of an automatic S-wave arrival time picking: a) Search for the maximum BK value from one seconds after the P-wave arrival time, b) Set-up of a time window with length of 50 samples before the maximum BK value, c) Assignment of S-wave phase arrival time with the sample point that the BK function starts to increase.

6. Final event declaration

Although P- and S-wave phase arrival time are determined in all stations, it could be mistake based on noise and false time (Fig 8a). In order to extract the mistaken arrival times, seismic traces of which P-wave arrival time and S-P time show linear are selected by using the Wadati diagram which plot P-wave arrival time and P-S time for velocity model. The main purpose of the Wadati diagram is to find origin time of event by plotting P-wave arrival time and S-P time recorded each traces. According to distance between station and hypocenter, plotting P-wave arrival time and S-P time show linear expressed by a first-degree equation. The mistaken phase arrival times are extracted when plotting P-wave arrival time and S-P time are out of linear in the Wadati diagram. When the number of traces included in around slope of the Wadati diagram by increasing y-intercept is maximum, P- and S-wave phase arrival times of these traces are selected (Fig 8b). In order to locate hypocenter the number of traces needs at least 3 of P- and S-wave phase arrival time. In this study the number of traces selects at least 6 of P- and S-wave phase arrival time extracted from the Wadati diagram to meet with linear. After the first event is declared by using the STA/LTA ratio method of CF, P- and S-wave arrival time are determined by using BK function. And accurate P- and S-wave phase arrival time are extracted from the Wadati diagram. Finally, when the number of traces determined accurate phase arrival times are 6 or more, the

final event is declared.



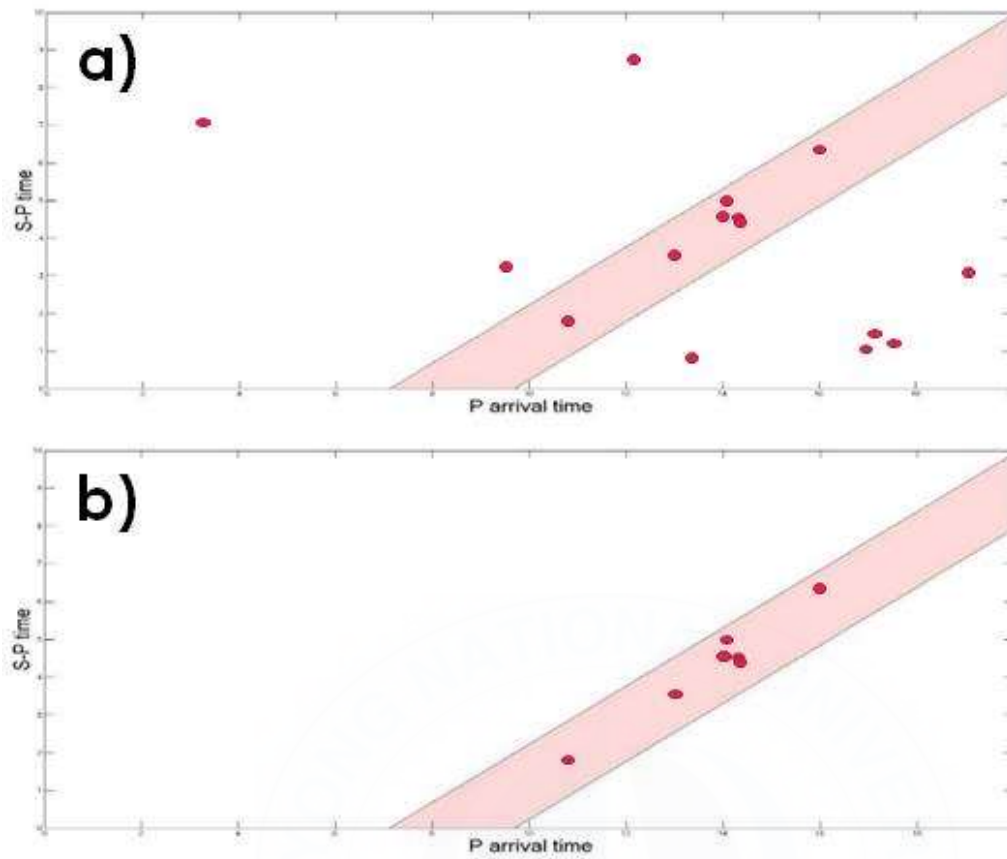


Fig 8. Use of the Wadati diagram for removal of falsely determined arrival time. a) S-P time against P-wave arrival time over all stations is plotted. b) The stations aligned in a zone with an average slope calculated using P- and S-wave velocity in the velocity model of the study area are selected as the ones with correctly determined arrival time.

III Data and result

1. Seismic network

The department of earth and environment sciences of Pukyung National University and the department of earth and environment science of Seoul National University have deployed a temporary broadband seismometer network which consists of 20 seismic stations in Jeju Island with spacing about 9 km since October 2013 (Fig 9). Table 2 represents information of 20 broadband seismic stations. Sampling rate is set up to 200Hz. The Korea Meteorological Administration (KMA) has detected 61 events in range of $33^{\circ} \sim 33.7^{\circ}$ latitude and $126^{\circ} \sim 127.1^{\circ}$ longitude since seismological observation (Fig 10). The first detected event occurred on 19 January 1986 and the last detected event occurred on 29 February 2016. Many events has occurred outside shoreline of Jeju island. Especially, dozens of continuous events happened in north sea of Jeju island on 15 August 2014. These events are applied to this method for detecting events and determining phase arrival times automatically. But data of 5 stations couldn't be used because of not saving data at this period. We use continuous data of 15 stations.

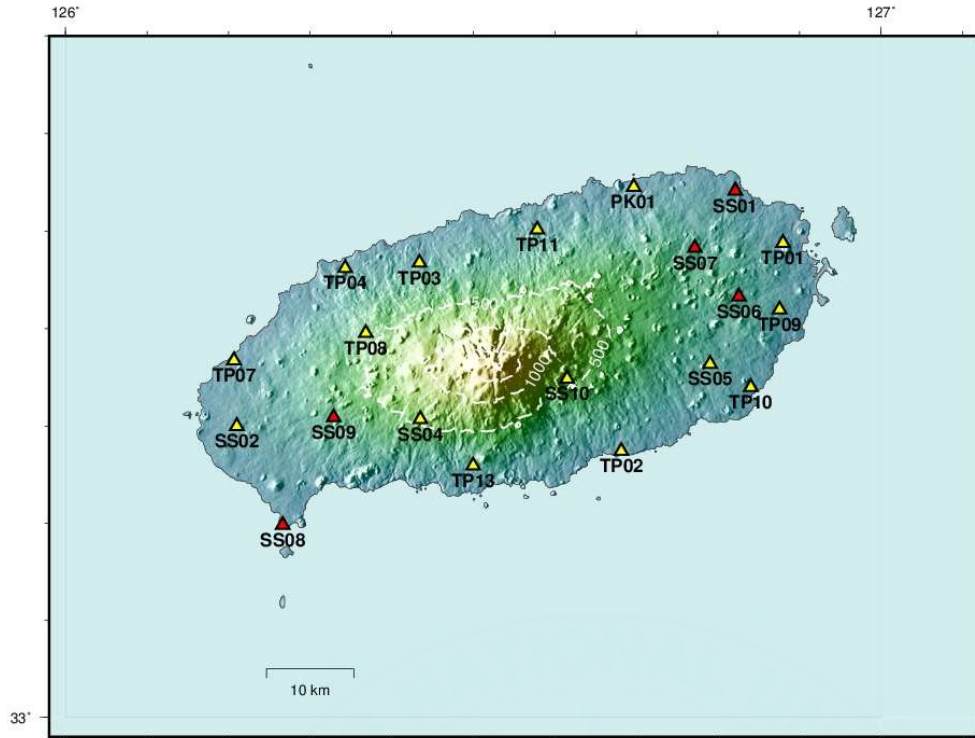


Fig 9. A temporary broadband seismograph network which is consisting of 20 stations distributed in Jeju Island. Yellow triangle shows the location of 15 stations used in this study and red one denotes 5 stations with no available data, respectively.

Station No.	Station Code	Latitude(°N)	Longitude(°E)
1	PK01	33.5453	126.6967
2*	SS01	33.5415	126.8213
3	SS02	33.3000	126.2100
4	SS04	33.3070	126.4350
5	SS05	33.3638	126.7903
6*	SS06	33.4330	126.8256
7*	SS07	33.4828	126.7717
8*	SS08	33.1983	126.2663
9*	SS09	33.3088	126.3288
10	SS10	33.3485	126.6151
11	TP01	33.4880	126.8797
12	TP02	33.2743	126.6816
13	TP03	33.4676	126.4341
14	TP04	33.4622	126.3429
15	TP07	33.3674	126.2066
16	TP08	33.3955	126.3682
17	TP09	33.4197	126.8756
18	TP10	33.3399	126.8404
19	TP11	33.5016	126.5785
20	TP13	33.2594	126.4999

Table 2. Station information. The stations with asterisk are not used in this study due to the recording problem.

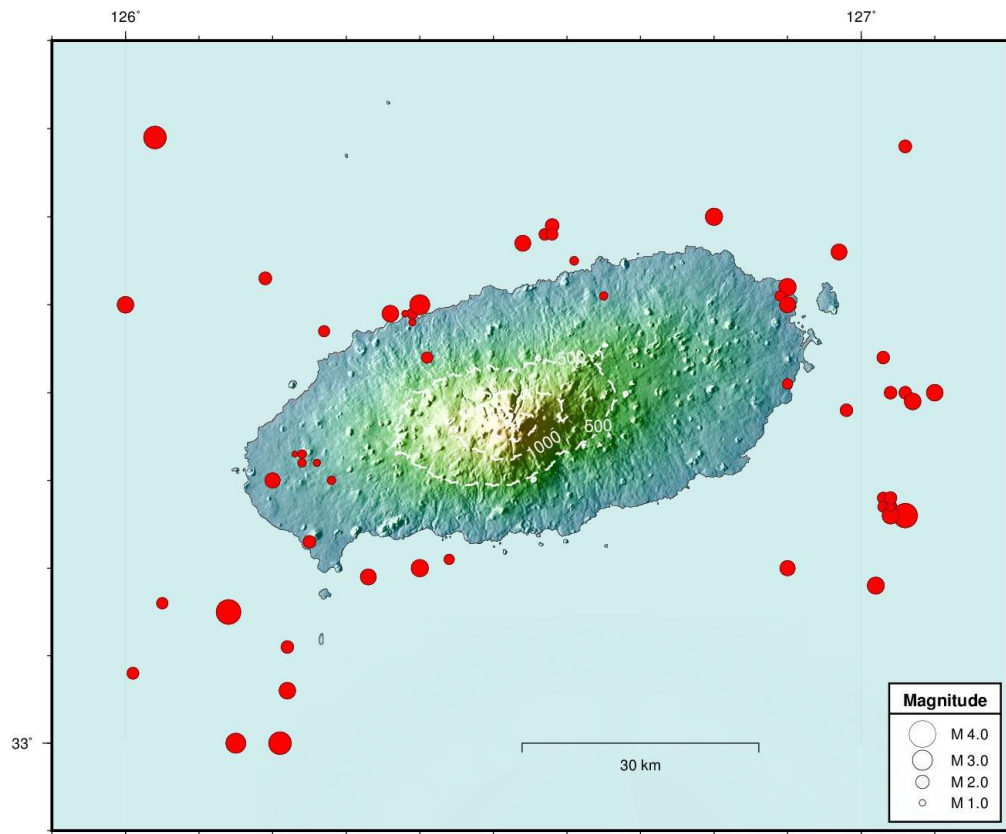


Fig 10. Events at a range of $33^{\circ} \sim 33.7^{\circ}$ in latitude and $126^{\circ} \sim 127.1^{\circ}$ in longitude announced by Korea Meteorological Administration.

2. Data

This method consist of 5 steps. First event declaration is carried out using STA/LTA ratio method of CF about a day data on 15 August 2014. Table 3 summarizes the parameters used for automatic detecting event and determining phase arrival times. Where T_{STA} and T_{LTA} are set up to 0.01s and 0.1s, respectively. The threshold and the criterion are set up to 15 and 3, respectively. The association window is set up to 6s. When first event is declared, 30s waveform is saved before 2s from point of event declaration. After automatic P-wave phase arrival time is determined by using BK function, the 3-axis rotation is applied by using the energy ratio of 3-components. Automatic S-wave phase arrival time is determined by using BK function in rotated waveform. The averaged slope of the Wadati diagram is calculated from manual P- and S-wave phase arrival time of 16 events in study area (Table 4). A slope and range of y-intercept are 0.77 and from -0.5 to 0.5, respectively. After declaring first event, the phase arrival times are determined. Final event is declared when the number of determination of phase arrival time, filtered with the Wadati diagram, are over 6. Total 30 events are declared automatically. But 3 events are false events because they include the other event in the saved waveform. As a result, seismic arrival times of 27 events are determined exactly (Table. 6).

Paramater		
Detecting	$T_{STA}(s)$	0.01
	$T_{LTA}(s)$	0.1
	<i>Threshold</i>	15
	<i>Criterion</i>	3
	<i>Associationwindow(s)</i>	6
Picking	<i>Slope</i>	0.77
	<i>Range of y-intercep</i>	-0.5 ~ 0.5

Table 3. Parameters for detecting event and picking arrival time.

Event No.	Origin time (UTC)		slope	Lat. (°N)	Lon. (°E)
	Date	Time			
1	2014-05-14	23:46:49	0.7721	32.8762	126.1359
2	2014-06-07	19:05:30	0.8325	33.5173	125.8868
3	2014-07-21	09:00:11	0.6201	33.3137	126.2409
4	2014-07-24	12:39:23	0.6340	33.4714	126.3900
5	2014-08-07	11:50:20	0.8379	32.9030	126.3220
6	2014-08-15	15:45:59	0.7772	33.5569	126.5843
7	2014-08-15	15:49:50	0.8285	33.5513	126.5896
8	2014-08-15	15:51:42	0.8055	33.5499	126.5889
9	2014-08-15	15:54:35	0.7671	33.5571	126.5889
10	2014-08-15	16:19:52	0.7903	33.5471	126.5891
11	2014-08-15	16:21:04	0.8293	33.5535	126.5868
12	2014-08-15	16:22:38	0.8680	33.5485	126.5873
13	2014-08-15	17:55:25	0.7672	33.5551	126.5863
14	2014-08-15	18:37:00	0.6874	33.5445	126.5892
15	2014-08-16	16:41:23	0.7522	33.4181	127.2082
16	2014-08-21	13:30:42	0.8068	33.8406	127.8950
Averaged slope			0.7735		

Table 4. The averaged slope of the Wadati diagram.

3. Determination of hypocenter

After P- and S-wave phase arrival time are determined, declared events are located by using Velellipse program for hypocenter determination (Kim et al., 2014). Hypocenter location is determined by using Velellipse program that find optimal velocity structure model to make the minimum RMS error of hypocenter location. The first velocity structure model consists of 12 layers of P-wave velocity. The S-wave velocity is determined as the optimal velocity model having a constant ratio of P-wave velocity. Table 5 represents the 12 initial P-wave velocity structure.

Table 6 shows the source parameters of 27 events located by using Velellipse program in north sea of Jeju island on 15 August 2014 (Fig 11). First event had happened at a quarter of fifteen (UTC) on 15 August 2014 and total 27 events was detected for about 9 hours. In order to locate hypocenter the number of used station is from the minimum of 6 stations to the maximum of 14 ones.

2 events (No. 5 and 6 in table 6) of total 27 events are detected by KMA and KIGAM. We compare the source parameters determined not only by this method, KMA, and KIGAM but also manual picking (Fig 12 and 13). Table 7 summarizes source parameters by means of each methods. Especially, This method and manual picking show similar results of source parameters. The seismic sources are determined by using Velellipse program of which input data are arrival time determined by this method and manual picking. The seismic sources

detected by KMA and KIGAM are determined by using other location program. The seismic sources determined by this method and manual picking show similar results of latitude, longitude and depth. Whereas, the seismic sources determined by this method and detected by KMA and KIGAM show a relatively large difference.



layer	depth(km)	Vp(km/s)
1	0~2	5.50
2	2~6	5.60
3	6~10	5.80
4	10~14	5.90
5	14~18	6.00
6	18~22	6.10
7	22~27	6.20
8	27~33	6.30
9	33~42	7.80
10	42~50	7.85
11	50~80	7.90
12	80~	8.00

Table 5. The 12 initial P-wave velocity structure.

Event No.	Origin time (UTC)	Lat. (°N)	Lon. (°E)	Depth (km)	RMS	Number of station
1	14:45:24.265	33.5474	126.5906	19.35	0.0511	6
2	14:49:59.960	33.5517	126.5872	13.36	0.0367	7
3	14:51:34.510	33.6515	126.6486	17.92	0.0780	7
4	15:45:59.470	33.5503	126.5861	12.42	0.0516	11
5	15:49:50.655	33.5458	126.5881	12.35	0.1296	14
6	15:51:42.235	33.5538	126.5853	13.74	0.0567	12
7	15:53:13.405	33.5629	126.5915	12.67	0.0469	11
8	15:53:55.965	33.5507	126.5870	14.14	0.0864	9
9	15:55:06.145	33.5719	126.5881	14.36	0.0482	8
10	15:57:48.355	33.5801	126.5944	14.04	0.0413	9
11	16:03:03.680	33.5639	126.5938	12.11	0.0755	7
12	16:07:17.895	33.5750	126.5866	14.96	0.0878	7
13	16:19:52.055	33.5482	126.5848	10.44	0.0663	11
14	16:20:21.140	33.5501	126.5878	12.59	0.0495	8
15	16:21:04.185	33.5686	126.5794	12.32	0.0790	12
16	16:21:41.330	33.5506	126.5851	12.74	0.0053	6
17	16:22:38.350	33.5641	126.5892	14.15	0.0880	13
18	16:26:01.900	33.5658	126.5932	14.00	0.0617	8
19	17:55:25.170	33.5655	126.5803	12.68	0.0912	13
20	18:08:09.220	33.5398	126.5894	14.31	0.0926	9
21	18:08:58.650	33.5611	126.5813	14.23	0.0706	10
22	18:38:00.240	33.5464	126.5888	11.53	0.0928	12
23	18:40:36.130	33.5627	126.5859	13.34	0.0829	13
24	18:41:33.325	33.5542	126.5863	12.14	0.0880	14
25	20:01:41.195	33.5590	126.5913	14.24	0.0441	7
26	21:00:02.670	33.5997	126.6101	18.73	0.0177	6
27	23:44:08.080	33.5660	126.5941	12.61	0.0439	7

Table 6. Source parameters of 27 events occurred in the northern offshore Jeju island on August 15, 2014.

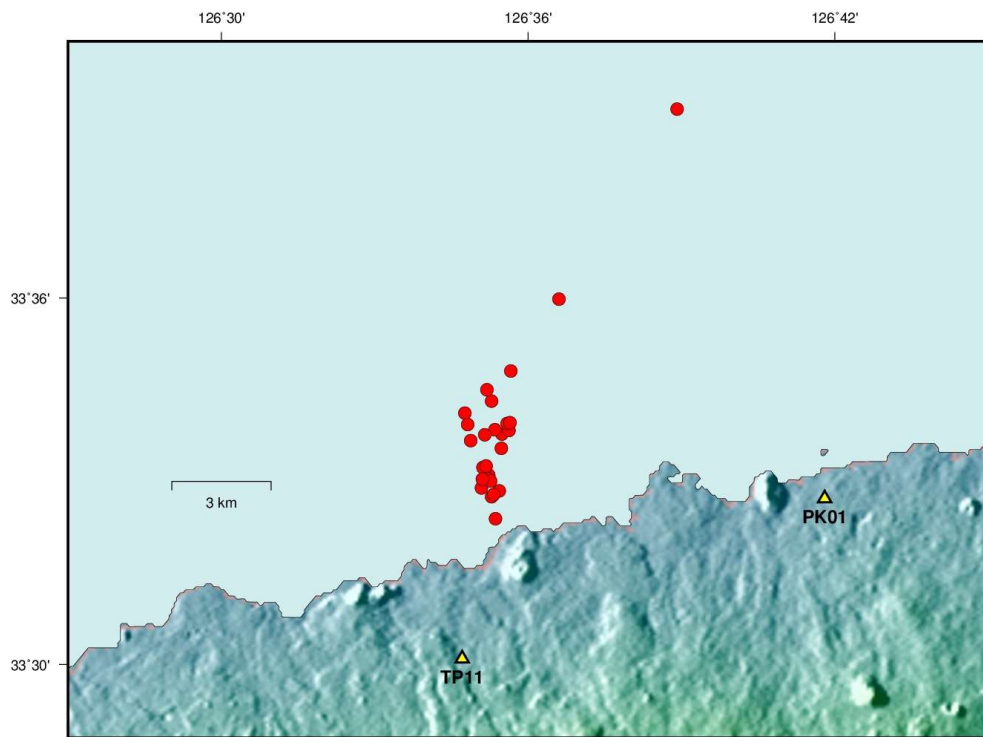


Fig 11. Earthquake sequence occurred in the northern offshore Jeju island on August 15, 2014.

	Event No.	Origin time (UTC)	Lat. (°N)	Lon. (°E)	Depth (km)	M _L	Distance difference (km)
KMA	1	15:49:50.000	33.5800	126.5800	-	1.74	3.876
	2	15:51:42.000	33.5900	126.5800	-	2.08	4.055
KIGAM	1	15:49:49.830	33.5616	126.5866	16.2	2.1	1.762
	2	15:51:41.960	33.5987	126.5829	4.5	2.4	5.017
Auto	1	15:49:50.655	33.5458	126.5881	12.35	-	0
	2	15:51:42.235	33.5538	126.5853	13.74	-	0
Manual	1	15:49:50.555	33.5501	126.5855	13.69	-	0.535
	2	15:51:42.095	33.5534	126.5887	14.85	-	0.318

Table 7. Comparison of source parameters announced by KMA and KIGAM with those determined using manual and automatic methods introduced in this study. Distance difference is a distance between epicenters determined using the automatic method and those using other methods.

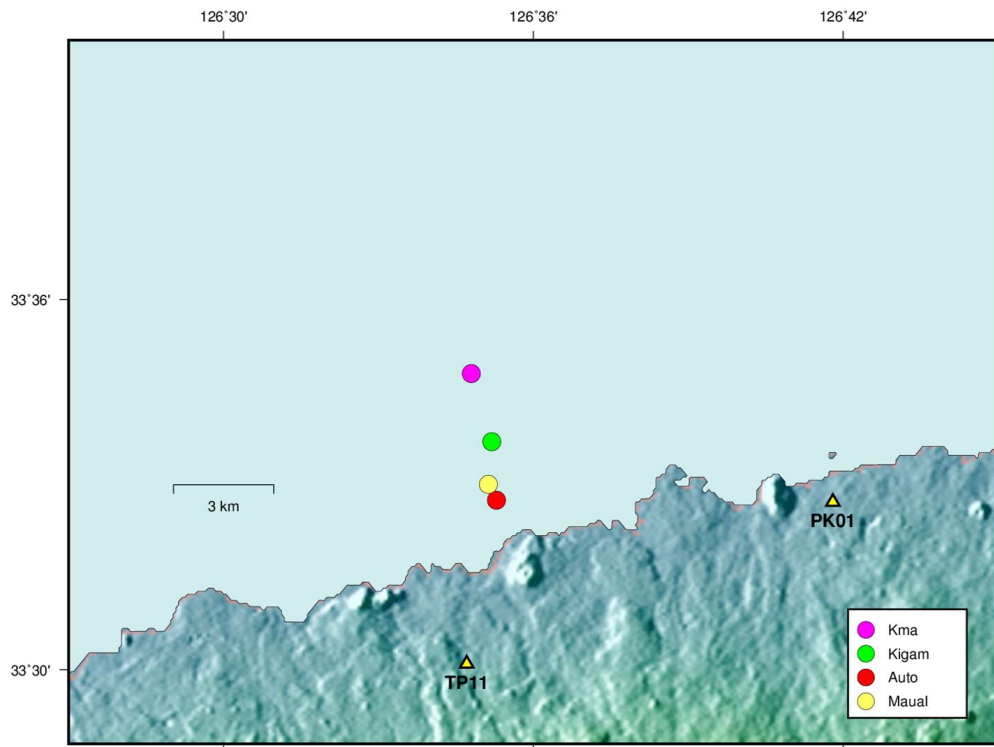


Fig 12. Comparison of the epicenters determined by KMA, KIGAM, and manual picking, respectively. The event is No. 1 at Table 7.

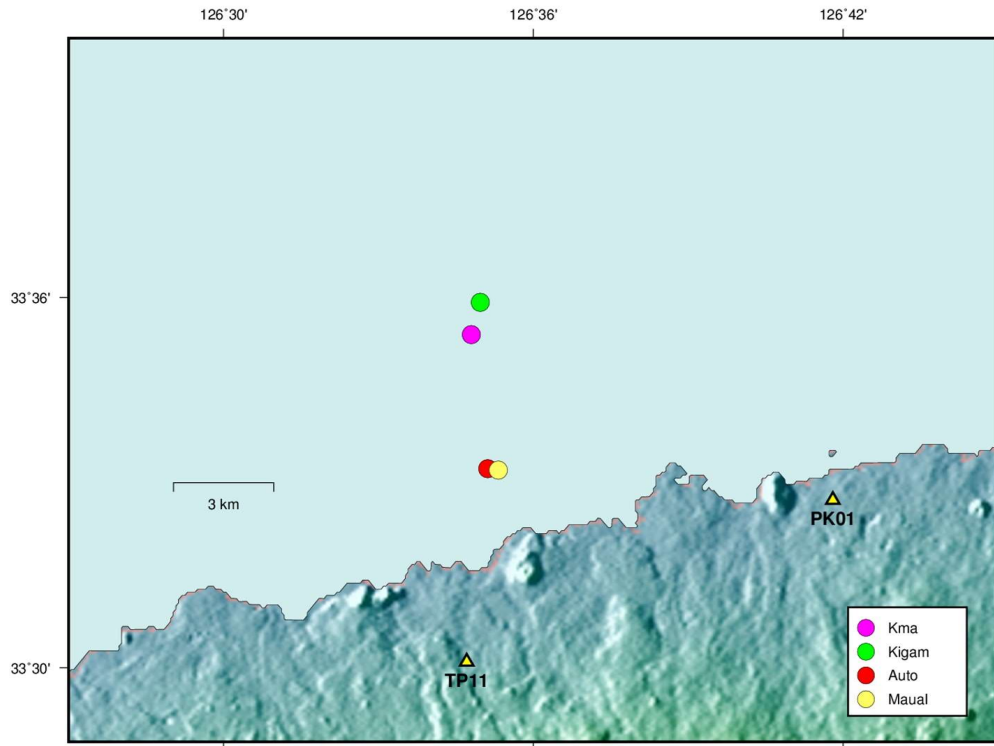


Fig 13. Comparison of the epicenters determined by KMA, KIGAM, and manual picking, respectively. The event is No. 2 at Table 7.

IV Discussion and Conclusion

We developed a method that consists of 5 steps in order to detect event and determine phase arrival times. In order to determine automatic phase arrival time, methods of ES, CF, and BK is applied to event data. Result of BK method shows the smallest residual time compared to ES and CF method. However, calculation of BK method has disadvantage that takes a long time rather than others. So, the CF method showing considerable variations when seismic phases arrive is used to detect event. After detect and save event waveform, phase arrival times are determined by using BK method. A number of pickers determine automatic P-wave phase arrival time. Whereas, this method determines not only P-wave phase arrival time but also S-wave phase arrival time automatically. Especially, in order to determine accurate S-wave phase arrival time traces are applied to 3-axis rotation by using the backazimuth and the incidence angle, which calculated by the energy ratio of 3-components. Also, new method extracting undistinguishable P- and S-wave phase out of linear expressed by a first-degree equation is applied and accurate P- and S-wave phase arrival times are only selected.

Numbers of continuous events happened in north sea of Jeju island on 15 August 2014. This method is applied to continuous data on 15 August 2014. First, 30 events are detected. However, because saved waveform of 3 events has other event, 27 events among them are

located by using Velellipse Program except 3 events. Then, the RMS error of 27 events shows reliable results. 2 events of total 27 events are detected by KMA and KIGAM. Source parameters of 2 events are determined by manual picking. We compare to source parameters which include not only ones announced by KMA and KIGAM but also ones determined manual picking and this method. Table 7 represents the source parameters of 4 methods. The seismic sources determined by this method and manual picking show similar results. Whereas, the seismic sources determined by this method and announced by KMA and KIGAM show a relatively large difference because of network size and algorithm difference of determining seismic source. The parameters of this method is similar to the parameters of manual picking. The distance difference between hypocenter of this method and one of KMA and KIGAM is about 3km. Whereas, The distance difference between hypocenter of this method and one of manual picking is about 0.5km. Because this method recognize little variation of amplitude, it tend to determining the earlier S-wave phase arrival time. So, event depth determined this method is shallow 1 more km than event depth determined manual picking.

In the process of locating hypocenter, waveform data from the minimum 6 to the maximum 14 is used. The source parameters of determined events summarizes in table 6. The RMS errors has values from about 0.02 to 0.12. We apply this method to continuous data on 15 August 2014 and the result show that microseismic analyst carried out with accuracy.

Reference

Akram, J. and Eaton, D. W., 2016, A review and appraisal of arrival-time picking methods for downhole microseismic data, *Geophysics*, 81, no. 2, KS67-KS871

Allen, R., 1978, Automatic earthquake recognition and timing from single trace, *Bulletin of the Seismological Society of America*, 68, 1521-1532

Allen, R., 1982, Automatic phase picker : their present use and future prospects, *Bulletin of the Seismological Society of America*, 72, S225-242

Baer, M. and Kradolfer, U., 1987, An automatic phase picker for local and teleseismic events, *Bulletin of the Seismological Society of America*, 77, 1437-1445

Chen, Z. and Stewart, R., 2006, A multi-window algorithm for real-time automatic detection and picking of p-phases of seismic events, *CREWES Research Report*, 18, 15.1-15.9

Earle, P. and Shearer, P., 1994, Characterization of global seismograms using an automatic-picking algorithm, *Bulletin of the Seismological Society of America*, 84, 366-376

Gutenberg, B. and Richter, C. F., 1956, Magnitude and Energy of

Earthquakes, *Annali di Geofisica*, 9: 1-15

Kendall, M., Maxwell, S., Foulger, G., Eisner, L., and Lawrence, Z.,
2011, Special section, Microseismicity: beyond dots in a box -
introduction, *Geophysics* 76, WC1-WC3

Kim, W., Hong, T.-K., and Kang, T.-S., 2014, Hypocentral parameter
inversion for regions with poorly known velocity structures,
Tectonophysics, 627, 182-192

Leonard, M. and Kennett, B.L.N., 1999, Multi-component autoregressive
techniques for the analysis of seismograms, *Physics of the Earth and
Planetary Interiors*, 113, 247-263

Lois, A., E. Sokos, N. Maratakis, P. Paraskevopoulos, and G. A.
Tselentis, 2013, A new automatic S-onset detection technique:
Application in local earthquake data, *Geophysics*, 78, no. 1, KS1-KS11

Maxwell, S., 2011. What does microseismic tell us about hydraulic
fractures?, SEG, Expanded Abstracts, 1565-1569

Molyneux, J. B., and D. R. Schmitt, 1999, First-break timing: Arrival
onset times by direct correlation, *Geophysics*, 64, 1492-1501

Munro, K., 2004, Automatic event detection and picking of P-wave
arrival, CREWES Research Report, 16, 12.1-12.10

Oye, V., and M. Roth, 2003, Automated seismic event location for hydrocarbon reservoirs, *Computers and Geosciences*, 29, 851--863,

Saari, J., 1991, Automated phase picker and source location algorithm for local distances using a single three component seismic station, *Tectonophysics*, 189, 307-315

Sabbione, J. I., and D. Velis, 2010, Automatic first-breaks picking: New strategies and algorithms, *Geophysics*, 75, no. 4, V67-V76

Wadati, K., 1933. On the travel time of earthquake waves, Part II, *Geophys. Mag.*, 7 : 101-111

Wong, J., Han, L., Bancroft, J., and Stewart, R., 2009, Automatic time-picking of first arrivals on noisy microseismic data, CSEG Conference Abstracts

Vera-Rodriguez, I., Bonnar, D., and Sacchi, M.D., 2011, Improvements in microseismic data processing using sparsity and non-linear inversion constraints, *CSEG Recorder*, 24-28

Yung, S. K., and L. T. Ikelle, 1997, An example of seismic time-picking by third-order bicoherence, *Geophysics*, 62, 1947-1952

지진파 위상 도착시간 자동 결정

김민욱

부경대학교 대학원 지구환경과학과

요약

P와 S파의 도착시간 결정은 미소지진 감지 및 지진원 요소 역산의 중요한 인자이다. 분석자가 수동으로 지진파 도착시간을 결정할 경우에 주관적인 판단에 따라 지진파형마다 일관성이 없는 도착시간을 결정할 가능성이 있으며, 이 과정에서 상대적으로 많은 시간이 소요된다. 이 연구에서는 자동으로 지진파 위상 도착시간을 결정하는 방법을 제시하고자 한다. 이 연구는 5가지 단계로 구성되어 있다. 첫 번째 단계는 연속파형에서 특성함수 (CF)를 이용하여 연속파형 자료에서 특성함수를 이용하여 최초 이벤트를 선언하는 것이다. 두 번째 단계는 정규화 포락 함수 (BK)를 이용하여 자동으로 P파 위상 도착시간을 결정하는 것이다. 세 번째 단계는 3성분의 에너지 비를 이용하여 3축 회전을 적용하는 것이다. 네 번째 단계는 자동으로 S파 위상 도착시간을 결정하는 것이다. 마지막 단계는 P파 도착시간과 S-P시간을 그래프로 나타내는 Wadati Diagram을 이용하여 잘못 결정된 도착시간들을 추출하는 것이다. 본 연구의 방법을 제주도 지역에 설치된 20개의 이동식 광대역 지진계로부터 얻어진 연속파형 자료에 적용하여 자동으로 이벤트 감지 및 위상 도착시간의 결정은 정확한 수행 결과를 보여주고 있다.